

The heat storage variability in the Brazil Current

Catherine B. Bou-Haya * and Olga T. Sato ¹

¹ University of São Paulo, Oceanographic Institute, São Paulo, Brazil, 05508-120

*Corresponding author: catherinebbh@hotmail.com

ABSTRACT

We investigated the variability of the oceanic heat storage on the western boundary of the South Atlantic Ocean. We aimed to understand the specific contribution of the Brazil Current as it travels southwards. The heat storage is evaluated near three latitudes, namely at 15°S, 24°S and 34.5°S. Numerical outputs of the oceanic potential temperature, salinity, and meridional components of the current's velocity resulting from the Estimating the Circulation and Climate of the Ocean (ECCO) model were used. We examined the time series of the heat storage from 1992 to 2015 for the three latitudes. The mean heat storage increased towards the south with a maximum at 24°S. At 34.5°S, there is a decrease in this property possibly due to its proximity to the Brazil-Malvinas Confluence. The Brazil Current's volume transport time series was correlated with the corresponding heat storage. The latitude that presented the highest correlation at interannual scale was 15°S with a value of 0.84 at a 95% of confidence level. The model outputs were also compared with *in situ* expendable bathythermograph measurements. Despite the presence of gaps and peaks indicating extreme events in the *in situ* data, both time series were statistically close and they showed similar mean annual cycles. No significant long-term HS trend was found at any of the three latitudes.

Keywords: Oceanic Heat Storage; Brazil Current; ECCO model; Interannual Variability; Volume Transport

INTRODUCTION

The South Atlantic Ocean plays an important role in the global climate system through both the wind-driven circulation of the upper layers and the revolving meridional patterns governed by the buoyancy flow due to the sinking waters at high latitudes. A striking mid-latitude feature in the ocean is the subtropical gyre whose circulation and velocity distribution are a result of the potential vorticity conservation. The basin-wide circulation, which is a persistent configuration in all basins, is the ocean's dynamical response to the relative vorticity

introduced by the large scale wind patterns (trade winds blowing at low latitudes and westerlies at mid-latitudes) and the effect that a spherical rotating planet impose onto a moving fluid. As a result, the large scale circulation has a northward flow in the South Atlantic's geostrophic interior and a western boundary current flowing southward to satisfy continuity conditions (Talley et al. 2011). Therefore, the South Atlantic subtropical gyre has an anticyclonic movement (counterclockwise). It is formed by the Brazil Current (BC) as the western boundary current, the South Atlantic Current (SAC) in the southern limit, the Benguela Current in the eastern boundary, and the South Equatorial Current (SEC) which closes the gyre at the northern limit (Peterson & Stramma 1991) (Figure 1).

Submitted: 25-Jan-2022

Approved: 30-Dec-2022

Associate Editor: Ilson Silveira



© 2022 The authors. This is an open access article distributed under the terms of the Creative Commons license.

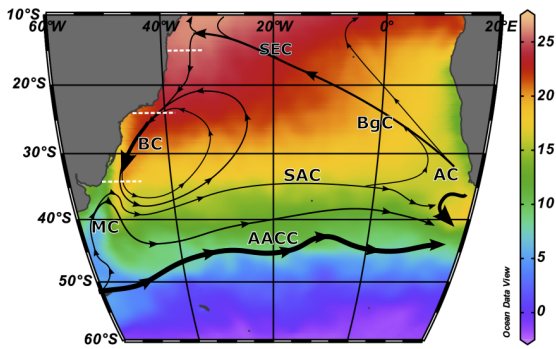


Figure 1. Schematic for the South Atlantic upper ocean circulation with the following currents: Brazil Current (BC), Malvinas Current (MC), South Atlantic Current (SAC), Agulhas Current (AC) retroflexion, Benguela Current (BgC), South Equatorial Current (SEC), Antarctic Circumpolar Current (AACC). The colors represent the mean sea surface temperature obtained from the World Ocean Atlas 2018 (WOA18). Adapted from Stramma & England (1999). The dashed lines represent the location of the transects examined in this study.

The western boundary current is narrower and much more intense compared to their counterparts around the gyre. These currents are determining elements for the mass and heat distribution in the subtropical gyres because they are responsible to transport heat from the tropical region towards the poles (Dunxin & Maochang 1991, Kelly & Dong 2004). In the South Atlantic, the bifurcation of the SEC in the Brazilian coast around 11°S gives rise of the southward flowing Brazil Current and the North Brazil Current, which flows northward carrying most of the water from SEC, while the volume transported southward only reaches about 4 Sv ($1 \text{ Sv} = 1 \times 10^6 \text{ m}^3 \text{ s}^{-1}$) (Stramma et al. 1990, Stramma & England 1999). Comparatively, the Brazil Current is not as intense as the Gulf Stream, the western boundary current of the North Atlantic subtropical gyre. After its formation, it only begins to reach greater depths much farther south, at 20°S (Stramma et al. 1990, Müller et al. 1998), when the current's transport reaches up to 6 Sv according to Peterson & Stramma (1991) compilation. From 24°S to 38°S , as the current travels along the South American continent, it shows a volume transport growth rate of 5% for 100 km, transporting around 19 Sv in the vicinity of 38°S

(Gordon & Greengrove 1986). Although the BC does not reach a velocity similar to its equivalent in the Northern Hemisphere (Gordon & Greengrove 1986, *ibid*), that increase in intensity is analogous to the one sustained by the Gulf Stream. The intensification is promoted by the presence of a recirculation cell in the Southwestern Atlantic. Furthermore, until it reaches 38°S , BC remains confined to the continental shelf along its route (Peterson & Stramma 1991). The region close to that latitude is known as the Brazil-Malvinas Confluence (BMC). There, the relatively warmer waters from the southward flowing BC meet the Malvinas Current, a western boundary current that carries cooler waters northward from the subpolar region (Garzoli & Garraffo 1989). The encounter of these two currents favor the formation of meanders and vortices (Gordon & Greengrove 1986). From that point, both currents move off the coast eastward as the South Atlantic Current.

From the thermodynamical point of view, the South Atlantic Ocean is the only basin among the global oceans which the meridional heat transport goes from the pole towards the Equator (Macdonald 1998, Garzoli & Baringer 2007, Garzoli & Matano 2011). That compensating flow occurs not only because there is the southward flowing North Atlantic Deep Water that exports heat to the Southern Hemisphere at depth but there is a large loss of latent heat through the surface at higher latitudes of the North Atlantic (Pfahl et al. 2014). The basic mechanism for the heat conservation in the oceans is described by the net surface heat flux being in balance with the amount of heat stored in the interior of the ocean and the divergence of the meridional heat flux. In a long-term scale, the oceanic heat storage (HS) should remain constant if the ocean was not subject to any heating or cooling trends. However, under the scope of a global warming effect due to anthropogenic actions, it has increased significantly during the years between 1955 and 1996 (Levitus et al. 2001). The Atlantic Ocean is the largest contributor to the escalation in heat storage with an increasing trend of 77 ZJ year^{-1} (1 ZT is 10^{21} J) in the upper 3000 m while it was 33 ZJ year^{-1} for the Pacific Ocean, and 35 ZJ year^{-1} for the Indian Ocean (Levitus et al. 2005).

One of the most important characteristics of the

ocean is its thermal capacity. Due to the water's high specific heat, energy can be stored in the fluid without increasing its temperature. Therefore, the ocean becomes an important regulator of the Earth's climate. The local heat storage in addition to the contribution advected by currents can be stored for a long period which makes the fluid work as a reservoir of energy (Levitus et al. 2000). Changes in HS may be a result of variability in various time scales, from intraseasonal to climate, having a direct influence on the heat transport in the ocean basins, as well as in the alteration of the energy balance that regulates the Earth's climate (Chambers et al. 1997, Levitus et al. 2001).

Another aspect that is no less relevant to HS is the fact that its variations may also indicate changes in the interaction between the ocean and the atmosphere. In this regard, the western boundary currents are important since they transport heat from the equatorial region to colder regions at higher latitudes. Dong & Kelly (2004) found that the amount of heat transferred from the ocean to the atmosphere is not only function of the magnitude of heat that was carried by the currents but also depends on the amount of heat that the ocean can store. Vivier et al. (2002), in turn, when studying the processes involving the heat balance in the Kuroshio Current region through a 3D finite element advection-diffusion model, observed that the HS inter-annual variations are essentially due to changes in the heat flux horizontal component due to advection and diffusion. Their results corroborated with Kelly & Dong (2004), where they concluded that the horizontal heat advection by the Gulf Stream is the main factor for the inter-annual variations of heat storage in the upper ocean layer.

It is important to highlight that HS has been more studied in ocean basins in the Northern Hemisphere. From *in situ* hydrographic data, HS can be estimated by integrating the potential temperature as a function of depth, times a scaling factor. Sonnewald et al. (2013) analyzed the variability of HS in the upper layer above 800 m of North Atlantic basin between 26°N and 36°N using data from the Rapid Climate Change (RAPID) project (Johns et al. 2011) which is located at the 26°N line, in addition to the use of data from Argo floats. Through analyzes made by box models, one of the conclusions was

that the non-seasonal heat storage variability (on a longer scale) in the subtropical regions is dominated by the ocean and not by the atmosphere.

Changes in HS are an important factor in the energy balance between the heat advected by the interior of the ocean and the budget at ocean-atmosphere interface. As a western boundary current, the BC is largely responsible for the poleward distribution of the oceanic heat. Changes in its volume transport could imply in changes in the heat transport, with consequences to the large scale subtropical circulation. Here we aim to investigate the variability of the Brazil Current's heat storage from seasonal to inter-annual scales. For that purpose, a time series of the current's velocity and physical parameters was necessary and outputs of the numerical model Estimating the Circulation and Climate of the Ocean (ECCO) (Forget et al. 2015) were used. A numerical model would allow us to isolate the contributions exclusively from the current's vertical and horizontal structure to the variations of the heat storage. Outputs from ECCO have been used by Piecuch & Ponte (2012) to study the rate of change of heat storage in the Atlantic Ocean, between 1993 and 2004 and to understand how it relates to changes in the ocean circulation. From the analysis and decomposition of the heat transport, they found that most of the interannual variation in the heat storage rate occurs in the upper layers of the ocean and that the major contributor to the heat budget in the region is the advection by currents. Most recently, the ECCO model was used to validate the BC volume transport estimation at 34.5°S obtained from hydrographic data and measurements from an array of pressure sensor inverted echo sounders (PIES) (Chidichimo et al. 2021).

In the following section we describe the model and the data used for the determination of the BC length at three specific locations along the Brazilian coast. In the methodology we discuss how we evaluated the best method to select the eastern limit of the BC for the HS estimations. In the Results section, we show the seasonal cycle of the HS at the three selected locations and the interannual anomaly time series. ECCO HS estimation was compared to the values estimated at 24°S, the only section where there were *in situ* measured temperature profiles.

DATA AND METHOD

The area of study covers the extension of the Brazil Current along the western boundary of the South Atlantic ocean, mostly concentrated near three latitudes, at 15°S, 24°S, and 34.5°S, Figure 1. The analyzed period spans from 1992 to 2015. Here we describe the data used.

We used the 4th version (v4r3) of the Estimating the Circulation and Climate of the Ocean (ECCO) model with outputs from 1992 and 2015 (Forget et al. 2015, Fukumori et al. 2017). The model has a spatial resolution of 1° × 1° and the temporal is monthly. The variables are the temperature (T), salinity (S) and the meridional current velocity (v) component. These fields were interpolated on to a 0.5° × 0.5° grid. The sections range from the surface to a reference level which was chosen by examining the transect at the selected latitudes. The BC western limit is the closest point to the coast and the eastern limit was estimated based on two criteria that will be explained shortly.

We examined *in situ* data acquired by the project "Monitoring of Regional Variability of Heat and Volume Transport in the Surface Layer of the South Atlantic Ocean between Rio de Janeiro (RJ) and the Ilha da Trindade" (MOVAR). This island is located at (20.5°S, 29.3°W). That monitoring line is part of the National Oceanic and Atmospheric Administration's (NOAA) Atlantic Oceanographic and Meteorological Laboratory (AOML) program which maintains several transects of XBTs along the Atlantic Ocean. It is also part of the Brazil's branch of the Global Ocean Observing System branch (GOOS-Brazil). Particularly, MOVAR's transect is located at 24°S between the continent and the Trindade Island where XBTs are launched during regular maintenance cruises from the Brazilian Navy. The XBT data for that transect is distributed through the website: <http://www.goosbrasil.org/movar>. The temperature time series of the ocean's upper layer (between surface up to approximately 700 m) were obtained from 2004 to 2015. These *in situ* sections were useful for the validation of the model's output, however when they were not available, the validation was done by comparing the model's outputs to the climatological mean from the World Ocean Atlas 2018 (WOA18) (Locarnini et al. 2019, Zweng et al. 2019). Goes

et al. (2019) have investigated the variability of the BC using the MOVAR time series to observe the seasonal and interannual changes. Therefore, we can rely on their findings to validate our model results at least in one our observed latitude lines, at 24°S.

WOA18 is maintained by NOAA and it is made available by the National Centers for Environmental Information (NCEI) on the website: <https://www.ncei.noaa.gov/access/world-ocean-atlas-2018/>. The long-term monthly mean, from 1955 to 2017, of temperature and salinity fields with a spatial resolution of 0.25° were available from that climatology. The MOVAR data were used in the comparison and validation of the model outputs at 24°S while the climatological data are used for the same purpose for all three latitudes.

DETERMINING THE WIDTH OF THE BRAZIL CURRENT

We examined the variability of the heat storage under the influence of the Brazil Current across three latitudes: 15°S, 24°S, and 34.5°S within the zonal range of 39.5°W–32°W, 47°W–36°W and 54°W–44°W, respectively. To bracket just the region of BC's influence, only the meridional component of the current's velocity was analyzed. As the BC flows southward, we can identify its presence through a flow parallel to the coast with negative values. However, its mean position relative to the coast can shift as a response to the strength of the subtropical gyre and the presence of mesoscale features, among other factors (Silveira et al. 2000). Therefore, for comparison purposes and to evaluate the sensitivity to the choice of the eastern limit of the BC, two criteria were tested: i) by finding the point where the maximum southward volume transport across the section is achieved, and ii) by analysing the average velocity in the water column.

The meridional volume transport (VT) across a zonal section is calculated as:

$$VT = \int_{-H}^0 \int_{x_1}^{x_2} v \, dx \, dz, \quad (1)$$

where H is a reference depth level (m), for instance, the level of no-motion, x_1 and x_2 are the zonal limits of the section, and v is the meridional component of the current (m s^{-1}). For the BC, the western limit

is chosen as the closest point to the coastline. The vertical reference level was chosen by examining the time series of the meridional velocity and the volume transport. At 15°S, the BC is mostly constrained above 150 m. For 24°S, the level of 600 m was chosen according to the updated compilation of BC meridional transport estimate by Cirano et al. (2006). For 34.5°S, the choice of the 800 m reference level was based on the work of Garzoli & Garraffo (1989).

Our aim is to compute the HS following the position of the BC. Due to fluctuations in the BC's width along the time series, the longitude of its eastern limit would change. The eastern limit is taken as the point where the flow changes direction, i.e., as one moves away from the coast, the southward flow would diminish and become northward, marking the outer limit of the BC influence. Using our first criterion, the point at which the volume transport reaches its maximum southward value was identified monthly at each section. Therefore, we tracked the lateral shifting of the BC over the years allowing us to evaluate its mean position and the standard deviation. In the second method, we examined the vertical mean of the meridional velocity at each grid point along each section over time. The longitude at which the mean meridional velocity changed signs was identified each month, that is, we identified the eastern point when the flow changed from south to north.

THE HEAT STORAGE

The oceanic heat storage is defined as:

$$HS = \rho C_p \int_{-H}^0 (T - T_m) dz, \quad (2)$$

where ρ is the density of the seawater (kg m^{-3}), C_p is the specific heat of the water at a constant pressure ($\text{J kg}^{-1} \text{ }^\circ\text{C}^{-1}$). The integration limit H is the lower limit of the current, T is the potential temperature ($^\circ\text{C}$) as a function of depth and T_m is the monthly mean potential temperature profile at each grid point also known as the temperature of reference (Chambers et al. 1997, Sato & Polito 2008). Both ρ and C_p are determined from potential temperature and salinity data but here we assumed to be constant for all latitudes of interest as they do not

vary significantly within the region ($\rho C_p \sim 4 \times 10^6 \text{ J m}^{-3} \text{ }^\circ\text{C}^{-1}$). Therefore, HS has units of J m^{-2} . In this study, we express HS zonally integrated across the Brazil Current, thus its unit becomes J m^{-1} .

For each section, the time series of the heat storage is obtained and the long-term trend was determined by linear regression. The significance of the trend was tested by comparing the mean and the standard deviation (STD) of the first and second halves of the time series. Then, the average annual HS cycle for the three latitudes was identified and analyzed. The interannual variability of the heat storage was analyzed by removing its respective mean annual cycle. In addition, to remove high frequencies from the series, a low-pass 19-month Butterworth filter (Roberts & Roberts 1978, Selesnick & Burrus 1998) was applied in all data sets.

After removing the mean annual cycle and applying a 19-month filter to the heat storage and volume transport time series, the Shapiro-Wilk test was performed to evaluate the normality of the distribution of the corresponding results (Kokoska & Zwillinger 2000). In statistical analysis, when at least one of the two variables being analyzed has a non-normal distribution ($p\text{-value} < 0.05$), it is more appropriate to use a non-parametric approach (Lehman et al. 2013). It was found that, for all three latitudes, both HS and volume transport series have a $p\text{-value}$ less than 0.05. Thus, all of them have a non-normal distribution.

THE MOVAR TIME SERIES

The MOVAR temperature time series spans the period between 2004 and 2015. The end year coincides with ECCO's output. The XBTs were launched at about 15 nm apart, and its transects reached longitudes away from the coast beyond the region in which the BC operates. However, the temperature sampling did not start close to the coast. Thus, to match the closest possible region between MOVAR and ECCO, the first longitude that both have in common as the western limit was chosen.

The *in situ* data needed a quality control. Hence, for each observed temperature profile, spurious values (resulted from possible measurement errors) were eliminated, as well as values that ranged outside the expected mean temperature ± 3 STD.

Moreover, as these data have a higher vertical resolution than that of the model, they were subsampled to every 10 m from surface to the reference level of that latitude.

It should be noted that, to calculate the heat storage, it is necessary to use the potential temperature or the conservative temperature and, consequently, salinity becomes necessary. The salinity data provided by the AOML comes from the World Ocean Atlas 2013, with a spatial resolution of 0.25° . Therefore, the observed temperature was converted to conservative temperature using Gibbs-SeaWater (GSW) Oceanographic Toolbox of TEOS-10 (McDougall & Barker 2011). The same procedure applied to ECCO's time series was performed in the MOVAR data.

The long-term trend including the whole series of HS at that latitude was examined. The significance of the fit was tested by comparing the mean and the standard deviation (STD) of the first and second halves of the series. Also, the mean annual cycle using the time series was identified. These dataset, like the mean annual cycle, were compared with data from the same period at 24°S from the ECCO model.

RESULTS AND DISCUSSION

In this section we clarify the following aspects of the study: how does the model's output compare with the climatological data, and how does the BC's volume transport and HS vary meridionally along the latitudes. After that, we examine the heat storage changes due to the BC from seasonal to interannual scales.

BRACKETING THE BRAZIL CURRENT

First, we evaluated the best criterion to identify the eastern limit of BC, provided a sensitivity test for the choices, analyzed the HS variability and, finally, made comparisons between ECCO and MOVAR data.

Comparison between ECCO and WOA18

We compared the T and S fields from the outputs of the ECCO model with the climatological monthly means from the WOA18. The WOA18 temperature

field was interpolated to match ECCO's spatial resolution and then converted to potential temperature. The following results include the analysis of the differences between the total mean T and S fields for some arbitrarily selected depths.

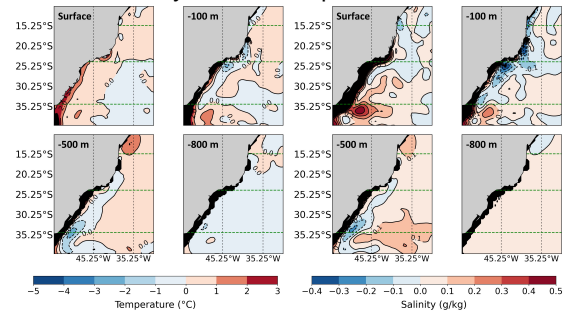


Figure 2. Difference (ECCO minus WOA18) between the mean temperature (two left panels) and salinity (two right panels) fields for different levels: surface, -100 m, -500 m and -800 m. The highlighted green horizontal dotted lines represent the latitudes of interest.

In the study region, the largest salinity disparities are found closer to the coast in the shallower levels of the water column. That result was expected given that these regions are subject to the coastal dynamics and mesoscale activities such as the discharge of the La Plata River and the BMC zone in the vicinity of 34.5°S . In addition, limited sampling and/or inconsistency of a near-shore data in the South Atlantic affects both WOA18 and ECCO. At the surface, the ECCO salinity field showed higher values closer to the southernmost latitude than the climatology which generated differences of approximately 0.5 g/kg . In the latitudes around 24°S , the variation between the model's output and the climatological field was around -0.1 g/kg to 0.2 g/kg at the surface. In the shallower region of 15°S , however, the WOA18 salinity exceeded that of ECCO, reaching differences up to -0.2 g/kg . Although at the depth of 100 m the disparities have occurred similarly to the previous level, as depth increases, the difference between the climatological data and the model output decreases which caused the differences to reach values between -0.1 g/kg to 0.1 g/kg at -800 m.

Regarding the temperature, the surface mean field from ECCO exhibited higher values compared to WOA18 in the vicinity of the studied latitudes, with a difference from -1°C to 2°C . South of 24°S

at -100 m depth, ECCO's outputs are warmer than WOA18 in a narrow band near the coast and the difference decreases as one moves towards the open ocean where it becomes slightly colder, by -1°C . At -500 m, there is a negative difference (up to -3°C) region centered near the latitude of 34.5°S which denotes that the ECCO is colder than WOA18. At -800 m, the largest differences are concentrated mostly near the coast.

The mean meridional velocity transects from ECCO as a function of longitude and depth depict the BC along the Brazilian coast, Figure 3. The shallowest section is found near the 15°S where the BC is confined above -150 m, over the continental shelf, Figure 3a. In Figure 3b, the BC is much deeper compared to 15°S . This agrees with Müller et al. (1998) where the BC reaches greater depths south of the latitude of 20°S . There, the mean velocity varies from -0.09 m s^{-1} closest to the shelf, up to the point where it changes sign at its eastern limit and a return flow starts, reaching values up to 0.03 m s^{-1} . At 24°S , it reaches depths around -600 m with a maximum of -0.09 m s^{-1} at the surface. At 34.5°S , Figure 3c, BC is even deeper than in 24°S , a factor that corroborates with the work of Garzoli & Garraffo (1989) and Stramma (1989). Gordon & Greengrove (1986) showed that, starting at 24°S the BC undergoes a strengthening and from 30°S the intensification is possibly due to the presence of a recirculation cell in the Southwest Atlantic. The 34.5°S transect is located closer to the northern limit of the BMC. Therefore, that latitude depicts a region with a strong mesoscale activity associated with it (Villas Bôas et al. 2015).

The Eastern Boundary of the Brazil Current

The position of the eastern boundary of the BC was estimated for each transect. This procedure was necessary to bracket the BC to ensure that just its variability was captured. Two distinct criteria were used for comparison and improvement of the accuracy in the determination: the volume transport and the mean velocity. It should be noted that the ECCO's velocity field has a higher vertical resolution at the upper layers while at the deeper layers the resolution decreases. This factor will be discussed subsequently, since it has a direct influence on the criteria used to identify the lateral limit of the current.

In Figure 4, it is notable the changes in longitude of the eastern edge of the current as a function of time at 15°S . Its mean position (in red) differs between the methods. The colored region shows the STD estimated using the monthly values. In the upper panel, the position where the eastern edge was determined from the point where the southward volume transport was maximum is shown. In the lower panel, the edge was determined where the mean meridional velocity averaged from surface to the lower limit of the BC was approximately null. Table 1 summarizes the results found for the eastern limit for each latitude through the two criteria used.

Table 1. The vertical (H) and the eastern (longitude) limits of the BC at each transect obtained from ECCO outputs. The longitudes are presented as the mean and standard deviation.

Latitude	H	Vol.Transport	Mean Velocity
15.0°S	-150 m	$(35.5 \pm 0.1)^{\circ}\text{W}$	$(37.1 \pm 1.0)^{\circ}\text{W}$
24.0°S	-600 m	$(38.2 \pm 0.1)^{\circ}\text{W}$	$(38.0 \pm 0.1)^{\circ}\text{W}$
34.5°S	-800 m	$(46.6 \pm 0.2)^{\circ}\text{W}$	$(46.5 \pm 1.1)^{\circ}\text{W}$

At 15°S when using the volume transport criterion, the mean longitude of BC's eastern boundary was $(35.5 \pm 0.1)^{\circ}\text{W}$. By using the average velocity criterion, the mean limit obtained was $(37.1 \pm 1.0)^{\circ}\text{W}$. In the latter, the STD is significantly greater, Table 1. This difference is due to the fact that the BC there occupies a shallow layers and the average speed at one specific point in upper layer would vary more in comparison to an integrated value such as the transport. Thus, the integrated effect decreases the variation imposed by the average speed in the column, which decreases the variation of the lateral boundary.

Another factor that potentially influences the identification of the eastern boundary at 15°S is that the region is closer to the point where the bifurcation of the South Equatorial Current occurs. The dynamics associated meridional displacement of the bifurcation position impact the determination of the lateral boundary of the BC, which can result in greater variations.

At 24°S , the eastern boundary found through the transport method was $(38.2 \pm 0.1)^{\circ}\text{W}$ while through the average speed criterion was $(38.0 \pm 0.1)^{\circ}\text{W}$,

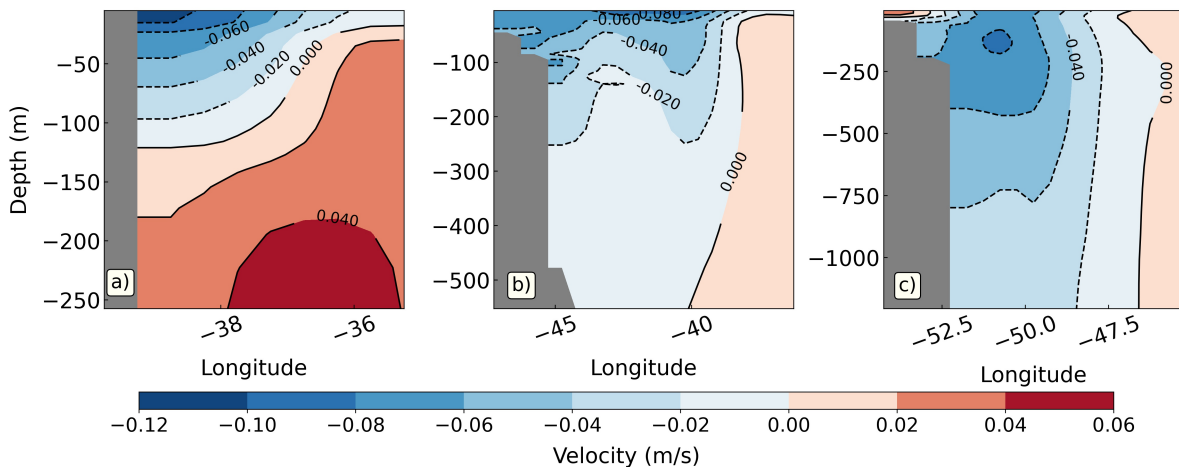


Figure 3. Zonal sections of the mean meridional velocity as a function of longitude and depth at the latitudes of: a) 15°S, b) 24°S and c) 34.5°S. The contours represent the current's velocity in m s^{-1} , the blue colors characterize the negative speeds (southward) and the more reddish colors, positive speeds (northward). Note that both the meridional and depth scales change for each panel.

Table 1. In this case, the mean and the STD from both methods are indistinguishable, indicating a more stable current. Hence, time series have, on average, the same pattern of variability in 24°S. Despite that latitude being located closer to a region with associated mesoscale dynamics, such as the formation of cyclonic vortices near 23°S (Campos et al. 1995, Calado et al. 2006), the ECCO's resolution is not high enough to resolve them. The results obtained here did not distinguish between both methods of selection. Either criteria were satisfactory.

At 34.5°S, the mean position obtained by the volume transport method was $(46.6 \pm 0.2)^\circ\text{W}$ and the average velocity method led to $(46.5 \pm 1.1)^\circ\text{W}$, Table 1. That latitude is located just north of the BMC region and it marked with the presence of oceanic fronts displaying strong gradients (reaching up to $1^\circ\text{C}/250\text{ m}$, according to Garzoli & Garraffo (1989) and an intense mesoscale disturbance activity (Gordon 1989). The encounter between the two currents does not happen at a fixed latitude over time, and it may vary seasonally (Meinen et al. 2017). The fact that 34.5°S is located close to the confluence possibly influences the average position of the BC. Similar to what was observed at 15°S, at 34.5°S the integrated transport minimized variations in the position of the lateral limit of the

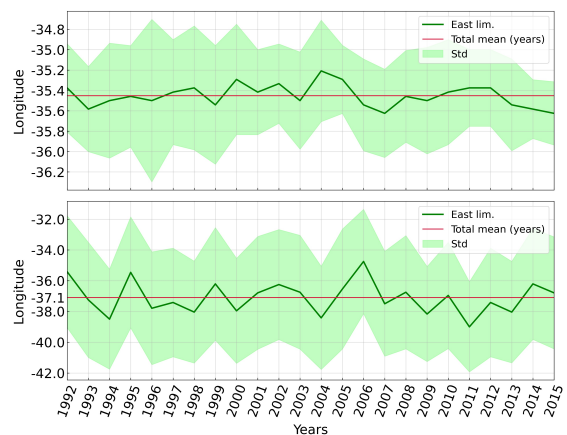


Figure 4. Longitude of the eastern limit of the BC at 15°S as a function of time, from 1992 to 2015, from ECCO outputs, using the volume transport criterion (upper panel) and the average speed criterion (lower panel). The red line represents the mean position eastern boundary, and the colored region is the STD.

BC over time, whereas, through the average speed at specific points may result in an increase in the STD.

The proximity with a shallower continental shelf, change in the coastline orientation, and the encounter with the Malvinas Current are some of the factors that may cause the formation of vortices and meanders by the BC (Signorini 1978, Campos

et al. 1995, Calado et al. 2006). Under that context, it is possible to explain the variations in the identification of the eastern boundary of the BC (Table 1). The transects at 15°S and 34.5°S are located in the vicinity of regions subject to intense large scale activity, therefore they might have influenced the choice for the mean eastern edge of BC. On the other hand, the latitude 24°S did not show these variations, producing more stationary results when using the criterion of volume transport or the average speed along the water column. Consequently, the volume transport criterion became most appropriate for the identification of the current eastern boundary.

The current is a dynamical phenomenon and presents seasonal and inter-annual variations, that is why we decided to evaluate the choice of the eastern edge by those two different methods. As the volume transport is an integrated variable, its calculation presented smaller standard deviations. As a result, that method proved to be a more adequate criterion for the identification of the lateral limit of the current, due to the fact that most of the values found per month are close to the average longitude found per year.

How sensitive is the HS estimation to the eastern boundary position's choice?

As shown above, the position of the eastern boundary of the Brazil Current varies over time. Therefore, we performed a sensitivity test to examine how the method of bracketing the BC would affect the heat storage estimation. First, for each latitude, the choice of a BC's easternmost position was made by averaging all the longitude values obtained previously (as shown in "Vol. Transport" column of Table 1) and used it as one fixed point. Conversely, the edge position that fluctuates in time obtained from the volume transport method was used. To illustrate the results, Figure 5 presents the heat storage (HS) obtained at 24°S . The HS was integrated from the coast up to the fixed point (blue line) while the red curve describes the same property considering the fluctuating point.

The standard deviation of HS when using the fluctuating point is substantially larger, $(2.48 \pm 0.13) \times 10^{16} \text{ J m}^{-1}$, than that of with fixed point, $(2.55 \pm 0.04) \times 10^{16} \text{ J m}^{-1}$. The larger variations

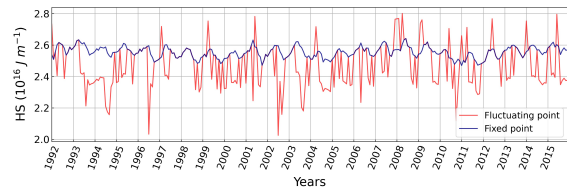


Figure 5. Integrated heat storage (HS) time series obtained at 24°S as a function of time, considering the eastern boundary of the Brazil Current as fixed at 38.2°W (blue) and as a fluctuating longitude (red).

are due to the current's lateral displacements away and closer to the coast. When using the eastern boundary as a fixed point, the region integrated in the heat storage becomes limited, thus all variations in HS comes from changes in temperature in the interior of the section. In other words, as the HS calculation involves the integration of the potential temperature in the water column, when considering a larger region, it is the same as adding to the calculation a high potential temperature per unit area. As a result, the HS curve integrated in the horizontal distance becomes artificially smoothed. Such considerations point out that for our objectives the most adequate form for calculating the heat storage is the use of the fluctuating point, which also considers the variations of the eastern boundary of the current over time.

HEAT STORAGE CHANGES IN THE BRAZIL CURRENT

First, we were interested in examining the annual cycle of HS at each transect then we investigated the interannual changes. For the HS annual cycle, at each grid point the vertical integral in equation 2 was calculated without taking into account the temperature of reference. Next we integrated that result zonally to obtain a time series of HS for each section and used it to examine the longer time scales. We observed that the heat storage showed a difference in phase of the annual cycle among the three latitudes (Figure 6). As HS is based solely on conservative temperature profiles which decrease to the south, one would expect that the HS would follow a similar pattern for meridional transects. However, HS is an integrated parameter that not only includes effects of the heat flux through the air-sea interface

but it is subject to the interior dynamics such as lateral advection, diffusion, convective mixing, instability, among others while the flow is advected southward by the western boundary. At 15°S, the minimum occurs in the month of July (winter), while at 24°S it occurs in September (transition between winter and spring) and, finally, at 34.5°S, the minimum takes place in February (summer). In turn, the highs occur in December and January (summer), January and April (summer and autumn) and July and September (winter and the transition from this to spring) for the latitudes of 15°S, 24°S and 34.5°S, respectively, Table 2.

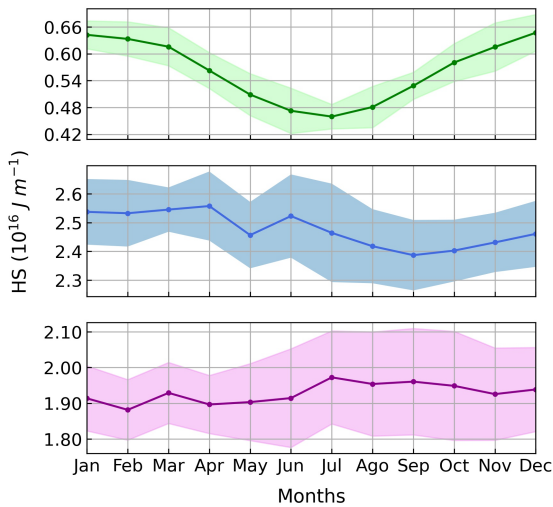


Figure 6. Mean annual cycle of the heat storage zonally integrated for the latitudes of 15°S (green), 24°S (blue) and 34.5°S (purple), from ECCO. The colored region for each panel is the STD.

Table 2. Mean annual cycle parameters of the zonally integrated heat storage at the three studied transects ($\times 10^{16} \text{ J m}^{-1}$).

Latitude	Minimum	Maximum	Mean	STD
15.0°S	0.46	0.65	0.56	0.07
24.0°S	2.39	2.56	2.48	0.06
34.5°S	1.88	1.97	1.93	0.03

Equation 2 calculations provide us with the interannual variability of the heat storage since the annual cycle is implicitly removed (Figure 7). We examined the long-term trends in the HS of each section by fitting a straight line in the whole HS time series. To evaluate the significance of the trends, we calculated the mean and the STD at each half of the HS time series, Table 3. These analyses

enabled us to conclude that the slopes differences found for the three latitudes were not significant.

Table 3. Mean and STD for the first and second half of the heat storage time series for the three transects ($\times 10^{16} \text{ J m}^{-1}$).

Latitude	1st half	2nd half
15.0°S	0.56 ± 0.08	0.56 ± 0.07
24.0°S	2.46 ± 0.13	2.48 ± 0.13
34.5°S	1.94 ± 0.12	1.91 ± 0.12

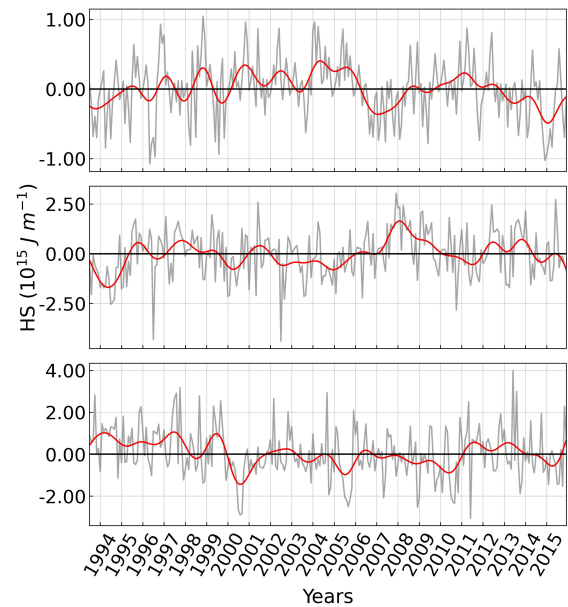


Figure 7. HS as a function of time (gray curve) and the 19-month filtered time series (red curves) for 15°S (top), 24°S (middle) and 34.5°S (bottom).

The resulting time series still presented high frequency noise, therefore we applied a 19-month filter for smoothing, Figure 7. We compared HS changes with that of the volume transport for each transect. Therefore, the mean annual cycle of the volume transport was removed from the original time series, and then it was smoothed out with the same filter as the HS. In Figure 7, HS is plotted (gray curve) simultaneously with the respective filtered time series (red curve). In Figure 8, the smoothed HS (red curve) and VT (blue curve) are presented. At 15°S, the HS varies between $-0.49 \times 10^{15} \text{ J m}^{-1}$ and $0.40 \times 10^{15} \text{ J m}^{-1}$. At 24°S the HS has a total range from $-1.69 \times 10^{15} \text{ J m}^{-1}$ to $1.95 \times 10^{15} \text{ J m}^{-1}$. At 34.5°S the HS ranges from $-1.44 \times 10^{15} \text{ J m}^{-1}$ to

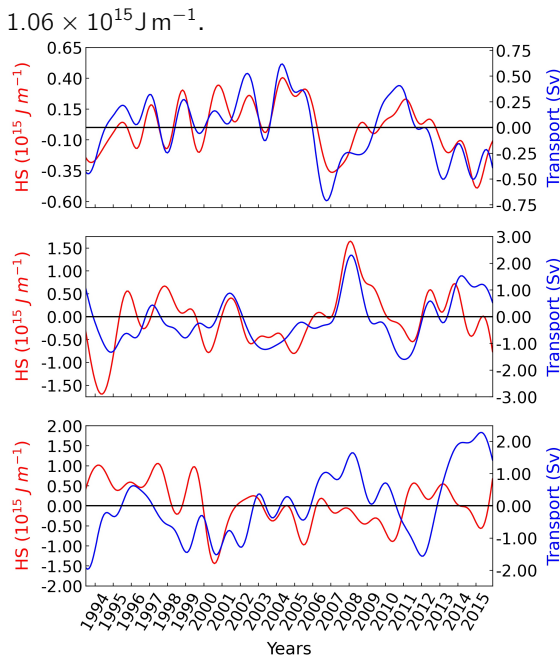


Figure 8. Smoothed HS and VT (red and blue curves, respectively) for latitudes of 15°S (top), 24°S (middle) and 34.5°S (bottom). HS units are J/m and VT is Sv, where 1 Sv is equal to $1 \times 10^6 \text{ m}^3 \text{ s}^{-1}$. The black horizontal line represents zero.

Since the Brazil Current moves southward (negative VT), positive anomalies represent a decrease in the transport in relation to its average, while the negative anomalies correspond to an increase in the current transport. Just for practicality, we are showing the BC's transport with a negative sign. In this way, a positive correlation between -VT and HS implies that both have the same pattern of increase/decrease, e. g., an increase in HS is related to an increase in the southward flow. Conversely, a negative correlation sets up an opposite pattern between the two parameters: if HS increases (decreases), the southward flow decreases (increases). Therefore, as can be seen in Figure 8, at 15°S, the HS anomalies fluctuates in phase with the BC's volume transport. The zero-lag correlation (r) of the filtered time series was confirmed statistically, being $r=0.84$ with a confidence level of 95%. At 24°S, the correlation between HS and -VT at this latitude was $r=0.56$, with the same level of confidence. Finally, at 34.5°S, the correlation, with a 95% confidence level, was -0.15, which was the lowest of all studied latitudes.

The works by Vivier et al. (2002) and Dong & Kelly (2004) found that the heat advection is the main responsible for the interannual variability of the heat storage of the ocean in the region of influence of the Kuroshio Current and the Gulf Stream. The scope of the present work does not include to explore the heat transport contribution, however we speculate that it is likely that it is also a strong influence for interannual variations in heat storage in the Brazil Current especially near the BMC region.

Comparison between ECCO and MOVAR

The heat storage time series of ECCO and MOVAR were calculated where they overlapped at 24°S, between 41°W and 37.5°W. The common time period between them is from 2004 to 2015. Figure 9 shows the zonally integrated HS in the transect.

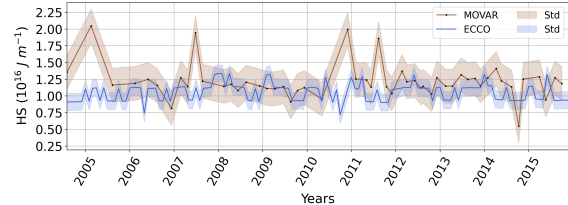


Figure 9. Zonally integrated heat storage at 24°S obtained from the ECCO model (blue curve) and the MOVAR project (brown curve). These curves include the annual mean cycle of HS. The shaded colored region represents the respective STD based on the monthly values.

The HS mean from MOVAR's time series is $(1.2 \pm 0.3) \times 10^{16} \text{ J m}^{-1}$. In turn, the ECCO's mean is $(1.1 \pm 0.1) \times 10^{16} \text{ J m}^{-1}$, its STD is smaller than the *in situ* observations. MOVAR's time series capture local fluctuations because it takes *in situ* instantaneous measurements, a feature that models not always are able to do. We can conclude that both series have the same magnitude on average. Positive values mean that the BC store heat locally which is expected since it is a western boundary current that redistributes heat towards the poles. In addition, the long-term trend for both data sets (not shown in the image) were calculated taking into account the mean and STD of the halves and found insignificant, as before.

The mean annual cycles of the *in situ* data sets and the model are shown in Figure 10. It is important to note that there was no temperature sampling

in all months for MOVAR, even though the study period is of 12 years. For this reason, a linear interpolation was performed on the MOVAR data and the result is represented by an open dot.

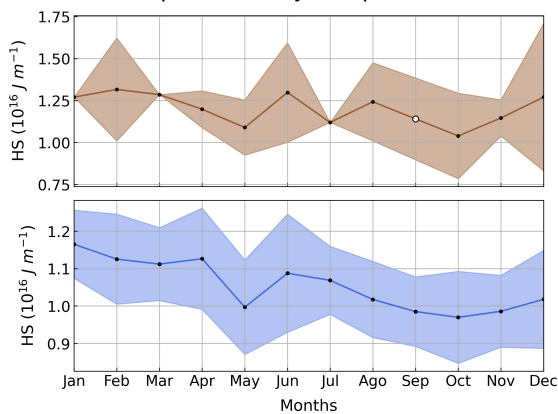


Figure 10. Mean annual cycle of the heat storage for the MOVAR data (top panel) and from ECCO's outputs (bottom panel), integrated up to -600 m. The monthly sample values represent the mean of all samples collected in that month. The open dot represents the linear interpolation made for the average annual cycle of the observed data, since there was no sampling in that period. The regions colored in brown (MOVAR) and blue (ECCO) represent the calculated standard deviation.

The HS annual cycle from MOVAR has an average of $(1.20 \pm 0.09) \times 10^{16} \text{ J m}^{-1}$, while the model has an average of $(1.05 \pm 0.06) \times 10^{16} \text{ J m}^{-1}$. The minimum observed for both the HS of the model and the observed data occurs in the month of October. The STD represent how far the values for each month have deviated from their respective mean. The main parameters of the annual cycle are listed in Table 4.

In addition to the fact that there was no sampling in all months for MOVAR, the XBT launches do not follow an exact parallel. Therefore, the regions limited to the HS calculation didn't have the same area, which may have caused some of the observed differences. The area of the region for HS calculation is a relevant factor and directly interferes with the final result. These analyses help us to conclude that ECCO model is able to reproduce the HS at the MOVAR site, with some limitations.

Table 4. Values of the average annual heat storage cycle for MOVAR and ECCO (in units of $1 \times 10^{16} \text{ J m}^{-1}$).

	Min.	Max.	Amplitude	Mean	STD
MOVAR	1.04	1.32	0.28	1.20	0.09
ECCO	0.97	1.16	0.19	1.05	0.06

CONCLUSION

This work aimed to study the variability of heat storage of the Brazil Current along the western boundary of the South Atlantic ocean using the outputs from the ECCO model. We examined three transects that bracket the BC at the latitudes of 15°S , 24°S , and 34.5°S . The period of study spans from 1992 to 2015. The model was validated relative to the climatological monthly mean data from the WOA18 and at 24°S , *in situ* data from a series of XBTs launched by the MOVAR project was used for comparison. To compute just the contribution from the current, the integral of the heat storage should be taken within the limits of the BC at the three latitudes. The selected criterion to bracket just the BC's contribution is where the meridional component of the southward volume transport is maximum. That criterion presented smaller standard deviations compared to the other method used (minimum mean velocity in the BC).

The annual mean of the heat storage had a maximum value at 24°S . In addition, the mean annual cycle has shifted phases among the three lines. At 34.5°S , the proximity to the Brazil-Malvinas confluence, a dynamically active region marked by intense formation of vortices and meanders and the intrusion of the cold Malvinas Current may impose a distinct annual cycle for the heat storage. In turn, the model indicated that the HS average annual cycle at 15°S and 24°S are seasonally driven, with the heat storage maximum happening in the months of warmer temperature.

The interannual variability was analyzed from the removal of the mean annual cycle from the HS time series, as well as with the usage of a 19-month low-pass filter. For the comparison, the same was done for the meridional volume transport time series. The correlation between these parameters was calculated for the three latitudes. At 15°S , the correlation coefficient r obtained was the highest of all. Although at that latitude the BC is influenced

by meandering systems, the variations of the transport to the south are strongly correlated with the variability of HS. At 24°S, that relationship occurs in a subtler way (r is moderate), but there is still a direct correlation between HS and VT. At 34.5°S, the correlation reverses sign and becomes significantly weaker, which suggests that, at that latitude, transport to the south no longer has as much influence on heat storage.

Finally, a comparison was made between the heat storage series of ECCO and that of MOVAR (between 41°W and 37.5°W, from 2004 to 2015). Although the time series of observed data peaks at certain times, both data sets remained in the same range of magnitude, approximately. The same occurred with the average annual cycles obtained, with the greatest storage of heat occurring in months of warmer temperatures. The minimum, in turn, occurred in the same month for both sets of data.

Our results showed that the ECCO model proved to be efficient for describing the mean and seasonal cycle of the heat storage associated with the BC flow. The values are statistically reliable when compared to the observed data at 24°S, a fact that motivates us to explore that model to represent the changes in the heat storage and volume transport along the western boundary current in the South Atlantic.

ACKNOWLEDGMENTS

We appreciate the reviewers for their valuable and constructive comments and suggestions. This study has been conducted using the ECCO v4r3 model developed by ECCO consortium <https://www.ecco-group.org/>. We also used data from the World Ocean Atlas 2018 (WOA18), which is maintained by NOAA and it is made available by the National Centers for Environmental Information (NCEI) on the website: <https://www.nodc.noaa.gov/OC5/woa18/>. The *in situ* data from the MOVAR Project is obtained from the <http://goosbrasil.org/movar/>. This study contributes to the SAMBAR Project funded by the Fundação de Amparo à Pesquisa do Estado de São Paulo (FAPESP), Brazil, under Proc. 2017-09659-6.

This study is a tribute to Dr. Affonso da Silveira

Mascarenhas Jr. He was OS's adviser for her M.Sc. degree in Physical Oceanography from the Oceanographic Institute of the University of São Paulo. He was the one who first introduced her to the importance of understanding the impacts of the South Atlantic circulation in a global climate sense. The role of the Brazil Current in the Sverdrup balance in the South Atlantic subtropical gyre was the focus of her thesis. He enthusiastically told her some about classical discussions on geophysical fluid dynamics he witnessed at the MIT and those ideas inspired her to pursue a Ph.D. in the US. Affonso was nice, funny, and a very authentic person!

AUTHOR CONTRIBUTIONS

C.B.B-H.: Formal analysis, Investigation, Methodology, Software, Validation, Visualization, Writing – original draft, Writing – review & editing.

O.S.: Conceptualization, Funding acquisition, Supervision, Project administration, Resources, Data Curation, Writing – review & editing.

REFERENCES

- CALADO, L., GANGOPADHYAY, A. & DA SILVEIRA, I. 2006. A parametric model for the Brazil Current meanders and eddies off southeastern Brazil, *Geophysical Research Letters* **33**(12), 1–5.
- CAMPOS, E. J., GONÇALVES, J. & IKEDA, Y. 1995. Water mass characteristics and geostrophic circulation in the South Brazil Bight: Summer of 1991, *Journal of Geophysical Research: Oceans* **100**(C9), 18537–18550.
- CHAMBERS, D. P., TAPLEY, B. & STEWART, R. 1997. Long-period ocean heat storage rates and basin-scale heat fluxes from topex, *Journal of Geophysical Research: Oceans* **102**(C5), 10525–10533.
- CHIDICHIMO, M. P., PIOLA, A. R., MEINEN, C. S., PEREZ, R., CAMPOS, E., DONG, S., LUMPKIN, R. & GARZOLI, S. 2021. Brazil Current Volume Transport Variability During 2009–2015 From a Long-Term Moored Array at

- 34.5°S, *Journal of Geophysical Research: Oceans* **126**(5), e2020JC017146.
- CIRANO, M., MATA, M. M., CAMPOS, E. J. & DEIRÓ, N. F. 2006. A circulação oceânica de larga-escala na região oeste do Atlântico Sul com base no modelo de circulação global OCCAM, *Revista Brasileira de Geofísica* **24**(2), 209–230.
- DONG, S. & KELLY, K. A. 2004. Heat budget in the Gulf Stream region: The importance of heat storage and advection, *Journal of Physical Oceanography* **34**(5), 1214–1231.
- DUNXIN, H. & MAOCHANG, C. 1991. The western boundary current of the Pacific and its role in the climate, *Chinese Journal of Oceanology and Limnology* **9**(1), 1–14.
- FORGET, G., CAMPIN, J.-M., HEIMBACH, P., HILL, C. N., PONTE, R. M. & WUNSCH, C. 2015. ECCO version 4: An integrated framework for non-linear inverse modeling and global ocean state estimation, *Geoscientific Model Development* **8**(10), 3071–3104.
- FUKUMORI, I., WANG, O., FENTY, I., FORGET, G., HEIMBACH, P. & PONTE, R. M. 2017. ECCO version 4 release 3, *Technical report*, Jet Propulsion Laboratory/NASA, Pasadena, CA, USA.
- GARZOLI, S. L. & BARINGER, M. O. 2007. Meridional heat transport determined with expandable bathythermographs—Part II: South Atlantic transport, *Deep Sea Research Part I: Oceanographic Research Papers* **54**(8), 1402–1420.
- GARZOLI, S. L. & GARRAFFO, Z. 1989. Transports, frontal motions and eddies at the Brazil-Malvinas Currents Confluence, *Deep Sea Research Part A. Oceanographic Research Papers* **36**(5), 681–703.
- GARZOLI, S. L. & MATANO, R. 2011. The south atlantic and the atlantic meridional overturning circulation, *Deep Sea Research Part II: Topical Studies in Oceanography* **58**(17), 1837–1847.
- GOES, M., CIRANO, M., MATA, M. & MAJUMDER, S. 2019. Long-Term Monitoring of the Brazil Current Transport at 22°S From XBT and Altimetry Data: Seasonal, Interannual, and Extreme Variability, *Journal of Geophysical Research: Oceans* **124**(6), 3645–3663.
- GORDON, A. L. 1989. Brazil-Malvinas Confluence—1984, *Deep Sea Research Part A. Oceanographic Research Papers* **36**(3), 359–384.
- GORDON, A. L. & GREENGROVE, C. L. 1986. Geostrophic circulation of the Brazil-Falkland confluence, *Deep Sea Research Part A. Oceanographic Research Papers* **33**(5), 573–585.
- JOHNS, W. E., BARINGER, M. O., BEAL, L. M., CUNNINGHAM, S., KANZOW, T., BRYDEN, H. L., HIRSCHI, J., MAROTZKE, J., MEINEN, C., SHAW, B. ET AL. 2011. Continuous, array-based estimates of Atlantic Ocean heat transport at 26.5°N, *Journal of Climate* **24**(10), 2429–2449.
- KELLY, K. A. & DONG, S. 2004. The relationship of western boundary current heat transport and storage to midlatitude ocean-atmosphere interaction, *Earth's Climate: The Ocean-Atmosphere Interaction, Geophys. Monogr* **147**, 347–363.
- KOKOSKA, S. & ZWILLINGER, D. 2000. *CRC standard probability and statistics tables and formulae*, Crc Press.
- LEHMAN, A., O'ROURKE, N., HATCHER, L. & STEPANSKI, E. J. 2013. *JMP for Basic Univariate and Multivariate Statistics: Methods for Researchers and Social Scientists, Second Edition*, 2nd edn, SAS Institute Inc., Cary, NC, USA, chapter Measures of Bivariate Association, 121–162.
- LEVITUS, S., ANTONOV, J. & BOYER, T. 2005. Warming of the world ocean, 1955–2003, *Geophysical Research Letters* **32**(2), 1–5.
- LEVITUS, S., ANTONOV, J. I., BOYER, T. P. & STEPHENS, C. 2000. Warming of the world ocean, *Science* **287**(5461), 2225–2229.

- LEVITUS, S., ANTONOV, J. I., WANG, J., DELWORTH, T. L., DIXON, K. W. & BROCCOLI, A. J. 2001. Anthropogenic warming of earth's climate system, *Science* **292**(5515), 267–270.
- LOCARNINI, R., MISHONOV, A., BARANOVA, O., BOYER, T., ZWENG, M., GARCIA, H., REAGAN, J., SEIDOV, D., WEATHERS, K., PAVER, C. & SMOLYAR, I. 2019. World Ocean Atlas 2018, Volume 1: Temperature, *NOAA Atlas NESDIS 81* 52.
- MACDONALD, A. M. 1998. The global ocean circulation: A hydrographic estimate and regional analysis, *Progress in Oceanography* **41**(3), 281–382.
- MCDUGALL, T. J. & BARKER, P. M. 2011. Getting started with TEOS-10 and the Gibbs Seawater (GSW) oceanographic toolbox, *SCOR/IAPSO WG 127*, 1–28.
- MEINEN, C. S., GARZOLI, S. L., PEREZ, R. C., CAMPOS, E., PIOLA, A. R., CHIDICHIMO, M. P., DONG, S. & SATO, O. T. 2017. Characteristics and causes of Deep Western Boundary Current transport variability at 34.5°S during 2009–2014, *Ocean Science* **13**(1), 175–194.
- MÜLLER, T. J., IKEDA, Y., ZANGENBERG, N. & NONATO, L. V. 1998. Direct measurements of western boundary currents off Brazil between 20°S and 28°S, *Journal of Geophysical Research: Oceans* **103**(C3), 5429–5437.
- PETERSON, R. G. & STRAMMA, L. 1991. Upper-level circulation in the South Atlantic Ocean, *Progress in Oceanography* **26**(1), 1–73.
- PFAHL, S., MADONNA, E., BOETTCHER, M., JOOS, H. & WERNLI, H. 2014. Warm conveyor belts in the era-interim dataset (1979–2010). part ii: Moisture origin and relevance for precipitation, *Journal of Climate* **27**(1), 27–40.
- PIECUCH, C. G. & PONTE, R. M. 2012. Importance of circulation changes to atlantic heat storage rates on seasonal and interannual time scales, *Journal of Climate* **25**(1), 350–362.
- ROBERTS, J. & ROBERTS, T. D. 1978. Use of the butterworth low-pass filter for oceanographic data, *Journal of Geophysical Research: Oceans* **83**(C11), 5510–5514.
- SATO, O. & POLITO, P. 2008. Influence of salinity on the interannual heat storage trends in the Atlantic estimated from altimeters and Pilot Research Moored Array in the Tropical Atlantic data, *Journal of Geophysical Research: Oceans* **113**(C2).
- SELESNICK, I. W. & BURRUS, C. S. 1998. Generalized digital butterworth filter design, *IEEE Transactions on signal processing* **46**(6), 1688–1694.
- SIGNORINI, S. R. 1978. On the circulation and the volume transport of the Brazil Current between the Cape of São Tomé and Guanabara Bay, *Deep Sea Research* **25**(5), 481–490.
- SILVEIRA, I. C. A. D., SCHMIDT, A. C. K., CAMPOS, E. J. D., GODOI, S. S. D. & IKEDA, Y. 2000. A corrente do brasil ao largo da costa leste brasileira, *Revista Brasileira de Oceanografia* **48**, 171–183.
- SONNEWALD, M., HIRSCHI, J.-M., MARSH, R., MCDONAGH, E. & KING, B. 2013. Atlantic meridional ocean heat transport at 26°N: impact on subtropical ocean heat content variability, *Ocean Science* **9**(6), 1057–1069.
- STRAMMA, L. 1989. The Brazil Current transport south of 23°S, *Deep Sea Research Part A. Oceanographic Research Papers* **36**(4), 639–646.
- STRAMMA, L. & ENGLAND, M. 1999. On the water masses and mean circulation of the South Atlantic Ocean, *Journal of Geophysical Research: Oceans* **104**(C9), 20863–20883.
- STRAMMA, L., IKEDA, Y. & PETERSON, R. G. 1990. Geostrophic transport in the Brazil Current region north of 20°S, *Deep Sea Research Part A. Oceanographic Research Papers* **37**(12), 1875–1886.

- TALLEY, L. D., PICKARD, G. L., EMERY, W. J. & SWIFT, J. H. 2011. *Descriptive Physical Oceanography: an introduction*, Academic press.
- VILLAS BÔAS, A., SATO, O., CHAIGNEAU, A. & CASTELÃO, G. 2015. The signature of mesoscale eddies on the air-sea turbulent heat fluxes in the South Atlantic Ocean, *Geophysical Research Letters* **42**(6), 1856–1862.
- VIVIER, F., KELLY, K. A. & THOMPSON, L. A. 2002. Heat budget in the Kuroshio Extension region: 1993–99, *Journal of Physical Oceanography* **32**(12), 3436–3454.
- ZWENG, M. M., REAGAN, J., SEIDOV, D., BOYER, T., LOCARNINI, R., GARCIA, H., MISHONOV, A., BARANOVA, O., WEATHERS, K., PAVER, C. & SMOLYAR, I. 2019. World Ocean Atlas 2018, Volume 2: Salinity, *NOAA Atlas NESDIS 82* 50.